Energy release model of compaction band propagation

J. W. Rudnicki

Department of Mechanical Engineering and Department of Civil and Environmental Engineering, Northwestern University, Evanston, Illinois, USA

K. R. Sternlof

Department of Geological and Environmental Sciences, Stanford University, Stanford, California, USA

Received 27 May 2005; revised 18 July 2005; accepted 22 July 2005; published 17 August 2005.

[1] The elastic strain energy released per unit advance of a compaction band in an infinite layer of thickness h is used to identify and assess quantities relevant to propagation of isolated compaction bands observed in outcrop. If the elastic moduli of the band and the surrounding host material are similar and the band is much thinner than the layer, the energy released is simply $\sigma_+ \xi h \epsilon^p$ where σ_+ is the compressive stress far ahead of the band edge, ξh is the thickness of the band and ϵ^p is the uniaxial inelastic compactive strain in the band. Using representative values inferred from field data yields an energy release rate of 40 kJ/m^2, which is roughly comparable with compaction energies inferred from axisymmetric compression tests on notched sandstone samples. This suggests that a critical value of the energy release rate may govern propagation, although the particular value is likely to depend on the rock type and details of the compaction process.
Citation: Rudnicki, J. W., and K. R. Sternlof (2005), Energy release model of compaction band propagation, *Geophys. Res. Lett.*, *32*, L16303, doi:10.1029/2005GL023602.

1. Introduction

[2] *Mollema and Antonellini* [1996] reported observations of tabular zones of localized compactive deformation without evident shear in the Navajo Sandstone formation of southern Utah. They called these structures compaction bands (CBs). Similar structures have been observed in other field locations, and *Sternlof et al.* [2005] have reported detailed measurements from CBs cropping out as extensive arrays in the Aztec sandstone of southeastern Nevada. Localized compaction has also been observed in laboratory axisymmetric compression tests on sandstones [*Olsson*, 1999; *Olsson and Holcomb*, 2000; *Baud et al.*, 2004; *Klein et al.*, 2001] and in simulations of bore hole breakouts [*Haimson*, 2001; *Haimson and Lee*, 2004; *Klaetsch and Haimson*, 2002]. There are a number of differences among the laboratory observations and between the laboratory and field observations. Nevertheless, all the observed structures are characterized by localized porosity reduction in a roughly tabular zone that forms perpendicular to the maximum compressive stress. In addition to their inherent interest as a mode of localized deformation in porous rock that has been recognized only recently, CBs have potential importance to applications because of their effect on permeability. Both field [*Sternlof et al.*, 2004; *Taylor and Pollard*, 2000] and laboratory measurements [*Holcomb and Olsson*, 2003; *Vajdova et al.*, 2004] have shown that the permeability for flow across CBs is as much as several orders of magnitude smaller than that of the surrounding (host) material. Consequently, the formation of CBs in subsurface porous formations can strongly affect applications involving the injection or withdrawal of fluids, such as petroleum production, CO_2 sequestration, contamination clean-up and aquifer management.

[3] Viewed as two-dimensional profiles in outcrops of Aztec sandstone, individual CBs are generally long (10s of meters), thin (a few centimeters) zones of grains compacted through inelastic processes of porosity loss, primarily grain fracture and rearrangement. These CBs appear to have propagated outward along planes roughly orthogonal to the direction of maximum remote compressive stress [*Sternlof et al.*, 2005]. Experimental efforts to induce compaction localization in sandstone cylinders under axisymmetric compression [*Olsson*, 1999; *Olsson and Holcomb*, 2000; *Baud et al.*, 2004; *Klein et al.*, 2001] have tended to produce zones of compaction that appear to occur nearly instantaneously across the width of the specimen indicating that propagation, if it occurs, does so rapidly. On the other hand, in triaxial simulations of bore hole breakouts in sandstone [*Haimson*, 2001; *Haimson and Lee*, 2004; *Klaetsch and Haimson*, 2002], the tips of features resembling CBs have been identified extending from elongated, slot-shaped breakouts. In order to examine band propagation in the laboratory *Vajdova and Wong* [2003] and S. Tembe et al. (Initiation and propagation of strain localization in circumferentially notched samples of two porous sandstones, submitted to Journal of Geophysical Research, 2005, hereinafter referred to as Tembe et al., submitted manuscript, 2005) conducted axisymmetric compression experiments on cylindrical specimens with an external, circumferential notch. In some cases, they observed compaction initiating at the notch and extending across the specimen in increments corresponding to small load drops.

[4] A critical element in reconciling different laboratory observations, differences between laboratory and field observations, and in making predictions for practical applications is a better understanding of conditions for propagation. Although theoretical studies [*Olsson*, 1999; *Issen and Rudnicki*, 2000, 2001; *Rudnicki*, 2002; *Detournay et al.*, 2003; *Rudnicki*, 2003; *Bésuelle and Rudnicki*, 2004; *Rudnicki*, 2004] have had some success in identifying stress conditions and material behavior that are favorable for CB formation, there is less understanding of the conditions for propagation or arrest. *Sternlof and Pollard* [2002] and

Copyright 2005 by the American Geophysical Union.
0094-8276/05/2005GL023602$05.00

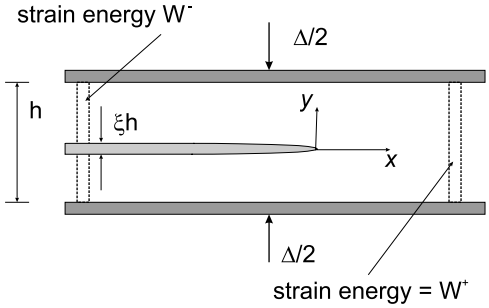

Figure 1. Model of a semi-infinite CB of maximum thickness ξh embedded in an infinite layer of thickness h. Boundaries of the layer are displaced toward each other by a total amount Δ. Propagation of the band a unit distance reduces the energy of a vertical slice far ahead of the band edge W^+ to that of a slice far behind the band edge W^-.

Sternlof et al. [2005] have suggested a linear elastic anticrack model for CB propagation. An anticrack is the compressive, closing-mode counterpart of the more familiar tensile, opening mode crack but with the sign of the stresses and crack-surface displacements reversed. Although the model formally predicts interpenetration of the crack surfaces, for CBs this interpenetration is interpreted physically as the inelastic compaction accompanying porosity loss. In this model, a CB propagates because of the compressive stress concentration at the edge of the band. Currently, little is known about the magnitude of the stress concentration required to induce propagation in either the field or laboratory. *Vajdova and Wong* [2003] and Tembe et al. (submitted manuscript, 2005) also used the anticrack model to interpret their experiments on notched specimens of Berea and Bentheim sandstone. From the nominal stress vs. displacement curves, *Vajdova and Wong* [2003] estimated a lower bound on the compaction energy for Bentheim of 16 kJ/m^2. Tembe et al. (submitted manuscript, 2005) estimated 43 kJ/m^2 for Berea, but because the band propagated at an angle of 55° from the plane ahead of the notch, it is likely to be a shear band.

[5] The stress at the edge of an anticrack is singular, as it is for a tensile crack. Consequently, the quantity relevant to the propagation of the band is the coefficient of the stress singularity, the stress intensity factor K, or, equivalently, the energy release rate $\mathcal{G}$, related to K by

$$\mathcal{G} = \frac{(1-\nu)}{2G} K^2 \tag{1}$$

where G is the shear modulus and ν is Poisson's ratio. At present the only estimates of critical values of K or $\mathcal{G}$ appear to be those by *Vajdova and Wong* [2003] and Tembe et al. (submitted manuscript, 2005) of compaction energies. In addition, it is unclear how these critical values relate to the parameters of the band, in particular, the inelastic compactive strain accommodated. This article presents a very simple energy release model of CB propagation as a framework for identifying the relevant controlling parameters.

2. Formulation

[6] The model is based on an example calculation of *Rice* [1968] illustrating the use of the *J*- integral and is shown in Figure 1. Physically, it represents an idealized geometry based on outcrop observations from the Aztec sandstone (Figure 2) [*Sternlof et al.*, 2005]. It consists of a long (infinite in the x-direction) layer of material of thickness h (in the y-direction). The layer contains a long (semi-infinite) CB which attains a fixed thickness ξh far behind the band edge. Both the layer and the band are uniform in the z-direction (orthogonal to the xy-plane of Figure 1), at least over distances much larger than h. The layer boundaries are then displaced toward each other a total distance Δ. The geometry constrains all displacements and strains to be uniaxial in the vertical (y) direction. Because the configuration is self-similar (translationally invariant in the x-direction), propagation of the CB a unit distance in the x-direction must reduce the strain energy in a vertical slice (perpendicular to the xy-plane) far ahead of the band edge to that of a vertical slice far behind the band edge. Because displacement is fixed on the boundaries of the sample, this difference in strain energy exactly equals the energy released per unit area swept out by propagation of the CB a unit distance.

[7] Far ahead of the band, the vertical strain is uniform and equal to Δ/h. If the material is assumed to be elastic, then the vertical stress is $M(\Delta/h)$ (horizontal stresses exist to enforce zero strain in these directions), where M is the modulus governing one-dimensional strain. For an isotropic material with shear modulus G and Poisson's ratio ν, $M = 2G(1-\nu)/(1-2\nu)$. The strain energy per unit area of a vertical slice far ahead of the CB is

$$W^+ = \frac{1}{2} Mh \left(\frac{\Delta}{h}\right)^2 \tag{2}$$

[8] Far behind the band edge, where the CB thickness is ξh, the strain is uniform in the CB ε_{band} and outside the

Figure 2. A typical configuration of three parallel CBs in the Aztec Sandstone, which forms the basis for the model illustrated in Figure 1. (left) The vertical slice with elastic strain energy W^- and (right) the vertical slice with energy W^+. (middle) The transitional zone associated with the elliptical taper of the central band's tip. In the photos, the hypothetical boundaries of the model layer surrounding the central band (Figure 1) fall between it and its two bounding neighbors, which are spaced 1.2 m apart. Thus, h in this case equals 0.6 m.

CB ε_{out}. The values are different but must be compatible with the total displacement of the boundary

$$\xi h\varepsilon_{band} + (1-\xi)h\varepsilon_{out} = \Delta \tag{3}$$

The stress outside the CB is given by $\sigma_{out} = M\varepsilon_{out}$. The material inside the CB is also assumed to be elastic, but with a different modulus M_b, and to have undergone an inelastic, vertical compactive strain ϵ^p. Hence, the stress is given by

$$\sigma_{band} = M_b(\varepsilon_{band} - \epsilon^p) \tag{4}$$

[9] Equilibrium requires that $\sigma_{band} = \sigma_{out}$. This equation can be combined with (3) to determine the strains in terms of Δ/h, the moduli, the geometry and ϵ^p. Therefore, the strain energy per unit area of a vertical slice far behind the edge of the CB is

$$W^- = \xi h\frac{1}{2}\sigma_{band}(\varepsilon_{band} - \epsilon^p) + (1-\xi)h\frac{1}{2}\sigma_{out}\varepsilon_{out} \tag{5}$$

Taking the difference $W^+ - W^-$ yields the energy release per unit area created of CB with thickness ξh:

$$\mathcal{G}_{band} = \frac{1}{2}\frac{Mh}{(M/M_b)\xi + (1-\xi)}\left\{\left(\frac{\Delta}{h}\right)^2\xi\left(\frac{M}{M_b} - 1\right) + 2\xi\epsilon^p\left(\frac{\Delta}{h}\right) - (\xi\epsilon^p)^2\right\} \tag{6}$$

3. Special Cases

[10] If the band modulus vanishes, $M_b = 0$, then (6) reduces to

$$\mathcal{G}_{band} = \frac{1}{2}\left[M\left(\frac{\Delta}{h}\right)\right]\Delta \tag{7}$$

where $\sigma_+ = M(\Delta/h)$ is the uniform stress ahead of the band. This is equivalent to the result for a crack with zero tractions on the surfaces and, notably, does not depend on the inelastic compactive strain. Equating (7) and (1) yields an expression for the stress intensity factor

$$K_{band} = \Delta\sqrt{\frac{MG}{(1-\nu)h}} \tag{8}$$

that is independent of the band length.

[11] If the elastic modulus of the CB remains the same as the material outside, $M_b = M$, then, neglecting the last term in the bracket, $(\xi\epsilon^p)^2$, (6) reduces to

$$\mathcal{G}_{band} = \sigma_+\xi\epsilon^p h \tag{9}$$

Thus, (9) has the simple interpretation of the stress multiplied by the compactive displacement in the CB.

[12] An indication of the effect of the difference in moduli can be obtained from $\mathcal{G}_{band}$ by simplifying the expression (6) for $\xi \ll 1$ and retaining only linear terms. The result is

$$\mathcal{G}_{band} = \left[M\left(\frac{\Delta}{h}\right)\right]\xi h\left\{\epsilon^p + \frac{1}{2}\left(\frac{\Delta}{h}\right)\left(\frac{M}{M_b} - 1\right)\right\} \tag{10}$$

Equation (10) suggests that the ratio of moduli is probably not significant unless it exceeds two and Δ/h is the same order of magnitude as ϵ^p. This result is consistent with the finding of Sternlof et al. (submitted manuscript, 2005) that the internal stiffness does not appreciably affect the state of stress around a highly eccentric ellipsoidal CB when ϵ^p is on the order of 10%. If the CB is modeled as a rigid inclusion, then $M_b \to \infty$, and the last parenthesis in (10) becomes -1. If the inelastic compactive strain is much greater than the nominal strain $\epsilon^p \gg \Delta/h$, then this reduces to the same expression as (9). Consequently, unless the stiffness of the CB material is much less than that of the surrounding material, (9) gives a good approximation to the energy release rate.

4. Discussion

[13] The simple model presented here suggests that CB propagation can reasonably be considered to occur when the energy released per unit advance of the band $\mathcal{G}_{band}$ is equal to some critical value $\mathcal{G}_{crit}$ that reflects the resistance of the material to compaction. Expressions (6), (7), (9), and (10) for $\mathcal{G}_{band}$ give the energy released in terms of the compactive strain of the band, the imposed strain, the elastic properties of the band and the surrounding material, and the thickness of the band and the surrounding material (spacing between bands). Assuming that band propagation does occur when $\mathcal{G}_{band} = \mathcal{G}_{crit}$, then it is possible to estimate the minimum value of the material parameter $\mathcal{G}_{crit}$ for representative values of the parameters derived from the Aztec sandstone [*Sternlof et al.*, 2005]. Taking $\sigma_+ = 40$ MPa, $\xi h = 0.01$ m, corresponding to 1 cm thick CBs spaced 1 meter apart, and $\epsilon^p = 0.1$, corresponding to a porosity reduction of 10%, gives $\mathcal{G}_{band} = 40$ kJ/m^2. $\mathcal{G}_{crit}$ must be at least this large at the end of propagation; otherwise the band would not have stopped propagating. Using the smallest and largest values for σ_+ estimated by *Sternlof et al.* [2005] (for the same values of ξh and ϵ^p) gives a range of $\mathcal{G}_{crit}$ from 10 to 60 kJ/m^2. For $M = 22$ GPa, corresponding to $E = 20$ GPa and $\nu = 0.2$, the value of σ_+ implies $\Delta/h = 1.8\times10^{-3}$. However, Δ is difficult to estimate and h, the CB spacing, is the most variable physical parameter in outcrop, ranging from millimeters to meters.

[14] Despite the many differences between the rock types, circumstances and morphology of band formation in the field and the laboratory, the range of values, 10 to 60 kJ/m^2, estimated from the field observations includes the two compaction energies inferred from the experiments on notched samples. The value of 40 kJ/m^2 inferred by Tembe et. al. (submitted manuscript, 2005) for Berea sandstone is in the middle of the range although, as noted earlier, the localized deformation in this case likely involved significant shear. The value of 16 kJ/m^2 inferred by *Vajdova and Wong* [2003] for Bentheim sandstone is a factor of 2.5 smaller. They did, however, report it as a lower bound. If $\mathcal{G}_{band} = 16$ kJ/m^2 and the stress is taken as 400 MPa, roughly

the axial stresses at propagation for the Bentheim samples, then (9) yields 0.04 mm for the compactive displacement. For a plastic strain of 7%, the porosity change estimated by *Klein et al.* [2001], the band width is 0.57 mm, about the same as observed by *Baud et al.* [2004, Figure 9]. Thus, the expression (9) gives results that are consistent with the limited data. To determine whether there is systematic variation of $\mathcal{G}_{\rm crit}$ with different porous sandstones and, perhaps, differences in the microscale processes of compaction (for example, fracturing vs. grain crushing) would require additional observations. Our results, however, indicate that the energy release rate is a reasonable framework for comparison.

[15] Since the term $\xi\epsilon^p h$ in this expression represents the net effective compactive displacement across the CB far behind the edge, an alternative criterion might be that propagation occurs at a critical value of this quantity. Because of the simplicity of the model, it is not specific about whether this inelastic strain (or compactive displacement) is accumulated in a small zone near the edge or more gradually over a large zone behind the edge. The model only assumes that it eventually reaches a constant, asymptotic value far behind the edge. Far ahead of the edge the stress is $\sigma_+ = M(\Delta/h)$. Far behind the edge the stress is

$$\sigma_- = M_b \frac{\Delta/h - \xi\epsilon^p}{\xi + (1-\xi)M_b/M} \tag{11}$$

Presumably, the stress increases from σ_+ far ahead of the CB edge to a higher value (theoretically infinite for the anticrack model) near the edge then decreases to σ_- at which point the inelastic strain has attained a critical value $(\epsilon^p)_{\rm crit}$. Further analysis of the spatial and temporal distribution of energy dissipation suggested by the more than 5 meters of elliptical taper near the ends of the bands reported by *Sternlof et al.* [2005] is warranted and should contribute to a better understanding of conditions for propagation.

[16] **Acknowledgments.** DE-FG-02-93ER14344 thanks Jim Rice for a suggestion concerning the model and Teng-fong Wong for discussion of his laboratory results. Principal financial support for this work was provided by the U. S. Department of Energy, Office of Basic Energy Science, Geosciences Research Program through grants to Northwestern University (DE-FG-02-93ER14344) and Stanford University (DE-FG03-94ER14462). Partial support during preparation of the initial manuscript while DE-FG-02-93ER14344 was a visitor at the Kavli Institute for Theoretical Physics was provided by the National Science Foundation under grant PHY99-07949. Preprint NSF-KITP-05-26. Additional support was provided to KRS by the Stanford Rock Fracture Project.

References

Baud, P., E. Klein, and T.-F. Wong (2004), Compaction localization in porous sandstones: Spatial evolution of damage and acoustic emission activity, *J. Struct. Geol.*, *26*, 603–624.

Bésuelle, P., and J. W. Rudnicki (2004), Localization: Shear bands and compaction bands, in *Mechanics of Fluid Saturated Rocks*, *Int. Geophys. Ser.*, vol. 89, edited by Y. Guéguen and M. Boutéca, pp. 219–321, Elsevier, New York.

Detournay, C., P. Cundall, and J. Parra (2003), A study of compaction band formation with the double yield model, in *FLAC and Numerical Modeling in Geomechanics: Proceedings of the Third International FLAC Symposium*, edited by R. Brummer et al., pp. 27–33, Swets & Zeitlinger, Lisse, Netherlands.

Haimson, B. C. (2001), Fracture-like borehole breakouts in high-porosity sanstone: Are they caused by compaction bands?, *Phys. Chem. Earth, Part A*, *26*, 15–20.

Haimson, B., and H. Lee (2004), Borehole breakouts and compaction bands in two high-porosity sandstones, *Int. J. Rock Mech. Min. Sci.*, *41*, 287–301.

Holcomb, D. J., and W. A. Olsson (2003), Compaction localization and fluid flow, *J. Geophys. Res.*, *108*(B6), 2290, doi:10.1029/2001JB000813.

Issen, K. A., and J. W. Rudnicki (2000), Conditions for compaction bands in porous rock, *J. Geophys. Res.*, *105*, 21,529–21,536.

Issen, K. A., and J. W. Rudnicki (2001), Theory of compaction bands in porous rock, *Phys. Chem. Earth, Part A*, *26*, 95–100.

Klaetsch, A. R., and B. C. Haimson (2002), Porosity-dependent fracture-like breakouts in St. Peter sandstone, in *Mining and Tunneling Innovation and Opportunity*, edited by R. Hammah et al., pp. 1365–1371, Univ. of Toronto Press, Toronto, Ont., Canada.

Klein, E., P. Baud, T. Reuschlé, and T.-F. Wong (2001), Mechanical behaviour and failure mode of Bentheim sandstone under triaxial compression, *Phys. Chem. Earth, Part A*, *26*, 21–25.

Mollema, P., and M. A. Antonellini (1996), Compaction bands: A structural analog for anti-mode I cracks in aeolian sandstone, *Tectonophysics*, *267*, 209–228.

Olsson, W. A. (1999), Theoretical and experimental investigation of compaction bands, *J. Geophys. Res.*, *104*, 7219–7228.

Olsson, W. A., and D. J. Holcomb (2000), Compaction localization in porous rock, *Geophys. Res. Lett.*, *27*, 3537–3540.

Rice, J. R. (1968), A path independent integral and the approximate analysis of strain concentration by notches and cracks, *J. Appl. Mech.*, *35*, 379–386.

Rudnicki, J. W. (2002), Conditions for compaction and shear bands in a transversely isotropic material, *Int. J. Solids Struct.*, *39*, 3741–3756.

Rudnicki, J. W. (2003), Compaction bands in porous rock, in *Bifurcations and Instabilities in Geomechanics*, edited by J. F. Labuz and A. Drescher, pp. 29–39, Swets & Zeitlinger, Lisse, Netherlands.

Rudnicki, J. W. (2004), Shear and compaction band formation on an elliptic yield cap, *J. Geophys. Res.*, *109*, B03402, doi:10.1029/2003JB002633.

Sternlof, K., and D. Pollard (2002), Numerical modeling of compactive deformation bands as granular anti-cracks, *Eos Trans. AGU*, *83*(47), Fall Meet. Suppl., Abstract T11F-10.

Sternlof, K. R., J. R. Chapin, D. D. Pollard, and L. J. Durlofsky (2004), Permeability effects of deformation band arrays in sandstone, *AAPG Bull.*, *88*, 1315–1329.

Sternlof, K. R., et al. (2005), Anti-crack inclusion model for compaction bands in sandstone, *J. Geophys. Res.*, doi:10.1029/2005JB003764, in press.

Taylor, W. L., and D. D. Pollard (2000), Estimation of in-situ permeability of deformation bands in porous sandstone, Valley of Fire, Nevada, *Water Resour. Res.*, *36*, 2595–2606.

Vajdova, V., and T.-F. Wong (2003), Incremental propagation of discrete compaction bands and microstructural observations on circumferentially notched samples of Bentheim sandstone, *Geophys. Res. Lett.*, *30*(14), 1775, doi:10.1029/2003GL017750.

Vajdova, V., P. Baud, and T.-F. Wong (2004), Permeability evolution during localized deformation in Bentheim sandstone, *J. Geophys. Res.*, *109*, B10406, doi:10.1029/2003JB002942.

J. W. Rudnicki, Department of Civil and Environmental Engineering, Northwestern University, Evanston, IL 60208–3109, USA. (jwrudn@northwestern.edu)

K. R. Sternlof, Department of Geological and Environmental Sciences, Stanford University, Stanford, CA 94305, USA. (kurtster@pangea.stanford.edu)